Eur. Phys. J. C 7, 655–667 (1999)
DOI 10.1007/s100529901036

THE EUROPEAN PHYSICAL JOURNAL C

New possibilities of old soft pomeron in DIS

P. Desgrolard[1], A. Lengyel[2], E. Martynov[3]

[1] Institut de Physique Nucléaire de Lyon, IN2P3-CNRS et Université Claude Bernard 43 boulevard du 11 novembre 1918, F-69622 Villeurbanne Cedex, France (e-mail: desgrolard@ipnl.in2p3.fr)
[2] Institute of Electronic Physics, National Academy of Sciences of Ukraine, 294015 Uzhgorod-015, Universitetska 21, Ukraine (e-mail: sasha@len.uzhgorod.ua)
[3] N.N. Bogoliubov Institute for Theoretical Physics, National Academy of Sciences of Ukraine, Metrologicheskaja 14b, 252143, Kiev-143, Ukraine (e-mail: martynov@bitp.kiev.ua)

Received: 9 June 1998 / Revised version: 27 August 1998 / Published online: 14 January 1999

Abstract. A traditional Regge model with a Q^2-independent Pomeron intercept closed (or equal) to one is constructed in order to describe the available data on the proton structure function. A Dipole Pomeron model which does not explicitly violate unitarity is developed and investigated. An excellent agreement with the 1209 data is found ($\chi^2/dof = 1.11$) in the whole kinematical domain investigated by experiments. A comparison of the model with already existing ones is made. The $x-$, Q^2-slopes and the effective intercept are discussed as Q^2 and x functions.

1 Introduction

The smooth transition between non-perturbative (soft pomeron and Reggeons) and perturbative (QCD evolution, hard pomeron) behaviour was studied and discussed in a number of original papers and reviews (*e.g.* [1,2]). Important questions remain, however, unresolved about the kinematical region (in Q^2, x-plane) in which the above approaches can be applied as well as about the region of their interference. In particular:

i) How large are the corrections to the DGLAP [3] evolution equation where the Q^2-evolution is usually considered in the leading $logQ^2$ approximation [4,5]?
ii) How large are the corrections to BFKL- or hard- pomeron [6]? What is their influence on the structure of the singularities in the j-plane, on the position of the rightmost singularity and on its intercept [4,5,7]?
iii) What do we know about unitarity in lepton-hadron Deep Inelastic Scattering (DIS)? How important are the shadowing corrections (SC) to the hard pomeron at small values of x [4,5,8,9]? Does the Froissart-Martin bound for hadronic total cross-sections remain valid for γp-interaction?
iv) What are the domains in Q^2 and x where a Regge description of the structure functions (SF) can be applied?

Detailed discussion may be found in the above quoted papers and references therein; here we briefly review the main conclusions known so far.

I) The experimental data on the deep inelastic SF are successfully described by the DGLAP evolution equation without any new ingredients [10–12] providing an initial structure function $F_2^{(0)} \propto x^{-\omega_0}$ at $x \to 0$ with $\omega_0 \approx 0.2-0.3$. We note that an important point in this approach is the choice of starting Q^2 value at which the input is defined. This value (usually $\sim 1-4$ GeV^2) is taken on a phenomenological ground and is justified *a posteriori*. At the same time in the HERA kinematical region the next order corrections are believed to be important [4,5]. From this point of view a good agreement of perturbative results with the data can be considered more strange than natural.
II) As shown recently [7], the correction $\delta\omega$ to the "Born" intercept of the BFKL Pomeron

$$\alpha_{\mathcal{P}}^{(0)}(0) - 1 = \omega_0 = 3N_c(\alpha_s/\pi)\ln 2 \approx 0.397,$$

calculated in the first order in $\alpha_s(\approx 0.15)$, is large and negative. More precisely, in accordance with estimates made in [7]

$$\omega = \omega_0 + \delta\omega \approx 0.0747 \quad \text{if} \quad \alpha_s = 0.15\ ,$$

$$\omega \approx 0.214 \quad \text{if} \quad \alpha_s = 0.081\ .$$

The authors of [7] conclude that the BFKL Pomeron and its next to leading approximation can be used only for rough estimates rather than for "precise" phenomenology.
III) Quantitative estimates of unitarity, shadowing corrections to structure functions as well as to parton distribution functions depend on additional assumptions within a specified procedure of unitarization. However, numerical estimates of SC originated from short distances show [8,13] that the effects are not small though they do not change qualitatively the behaviour of structure functions at least at moderate Q^2 and when

$x \lesssim 10^{-2}$. As for the unitarity condition in DIS, there is a common belief that the Froissart-Martin bound can not be proved for a process including "external" off-mass-shell particles. Nevertheless, as shown in [14], some restrictions on the values of the intercepts can be obtained on the ground of unitarity. We shall return to this subject below.

IV) In accordance with a widely accepted point of view, a soft contribution to the proton structure function F_2^p dominated by the pomeron works only at small Q^2. The basis of this belief is that at fixed Q^2 (larger than a few units of GeV^2) a *simple* fit (without any subasymptotic term which could be important here) gives $F_2^p \sim x^{-\delta}$ where $\delta \approx 0.2 - 0.4$ and δ is rising with Q^2.

The visible dependence of δ on Q^2 was used in the CKMT [15] and ALLM models [16,17] where a pomeron with an intercept depending on Q^2 was introduced.

Besides, a two pomerons model [18] and other models were proposed which smoothly interpolate between a soft and a hard Q^2-dependence [19] or combine these behaviours [20]. Of course, such a picture for the pomeron does not correspond to a true Regge singularity. It contradicts the main properties of simple Regge poles, namely factorization and universality (we mean that the "pomeron propagator" $(-is/s_0)^{\alpha_{\mathcal{P}}(t)}$ does not depend on external particles coupled with pomeron). Rather it can be considered as an effective contribution taking into account possible multipomeron exchanges. It would be interesting and important to find a justification by directly summing the multipomeron terms for example by an eikonal or a quasieikonal method.

Let us come back to the result of [14]. Because of unitarity, two kinds of singularity of the amplitude are possible: Regge singularities, those trajectories $\alpha(t)$ are, naturally, Q^2-independent; and Renormalization Group singularities which can depend on Q^2. From unitarity, the inequality

$$\alpha(Q^2) - 1 < \alpha(0) - 1$$

follows.

In spite of the above mentioned belief on the validity of a "non-hard pomeron" description of DIS data, restricted to small and moderate Q^2, many models of a soft pomeron contribution to F_2^p [20–25] were constructed and proved to be successful at small x ($\lesssim 10^{-2}$) and in a wide region of Q^2.

It is interesting to note that in most of them

$$F_2^p(x,Q^2) \underset{x\to 0}{\longrightarrow} f(Q^2)\ln(\frac{1}{x}) \cong f(Q^2)\ln W^2,$$

where

$$W^2 = Q^2(\frac{1}{x} - 1) + m_p^2$$

(m_p is the proton mass). Such a behaviour corresponds exactly to the contribution of a double j-pole $f(Q^2)/(j-1)^2$ to the partial amplitude of $\gamma^* p \longrightarrow \gamma^* p$, where $f(Q^2)$ is the residue function of the given reggeon (or pomeron). In hadronic models for elastic scattering, this singularity is known as a Dipole Pomeron (DP) with a trajectory $\alpha_{\mathcal{P}}(t)$, having unit intercept, $\alpha_{\mathcal{P}}(0) = 1$. As was shown in [26,27] the Dipole Pomeron model gives rise to the "best" description (in sense of χ^2) of the experimental data on the total cross section and $\rho-$ratio for nucleon-nucleon scattering (pp and $\bar{p}p$) as well as for meson-nucleon.

All this leads support to our present efforts to answer the following question. Is it possible, keeping a pure Regge picture, to extend the area of validity of the soft pomeron?

Taking into account the results of different "soft" models successfully applied at small [21,22,24,28] and at moderate Q^2 [21–24] one expect that the main difficulty should be the description of the data at large x rather than at large Q^2.

2 The model

As natural in a Regge approach, we deal with amplitudes and cross-sections rather than with structure functions. Therefore, we start from the expression connecting the transverse cross-section $\sigma_T(W,Q^2)$ for the (γ^*,p) process to the proton SF $F_2^p(x,Q^2)$

$$\sigma_T^{\gamma^* p}(W,Q^2) = \frac{4\pi^2\alpha}{Q^2}\frac{1}{1-x}(1+\frac{4m_p^2x^2}{Q^2}) \times \frac{1}{1+R(x,Q^2)}F_2(x,Q^2)\ , \qquad (1)$$

where we recall the negative squared four-momentum transfer carried by the virtual photon Q^2, the Björken variable x and the center of mass energy of the $\gamma^* p$ system W obey the condition

$$W^2 = Q^2\frac{1-x}{x} + m_p^2\ ;$$

here α is the fine structure constant and

$$R(x,Q^2) = \frac{\sigma_L(x,Q^2)}{\sigma_T(x,Q^2)}.$$

Unfortunately, the longitudinal cross-section σ_L is poorly known and one only knows that $R(x,Q^2)$ is small (at least at small Q^2 and x). In what follows we approximate

$$R(x,Q^2) = 0,$$

(*i.e.* the total and transverse cross-sections are supposed to be the same). Thus, we use the expression

$$F_2^p(x,Q^2) = \frac{1}{4\pi^2\alpha}a(x,Q^2)\sigma_T^{\gamma^* p}(W,Q^2)\ , \qquad (2)$$

with

$$a(x,Q^2) = \frac{Q^2(1-x)}{1+4m_p^2x^2/Q^2}. \qquad (3)$$

From the optical theorem

$$\sigma_T^{\gamma^* p}(W,Q^2) = \Im m\left[A(W^2,t=0,Q^2)\right] \qquad (4)$$

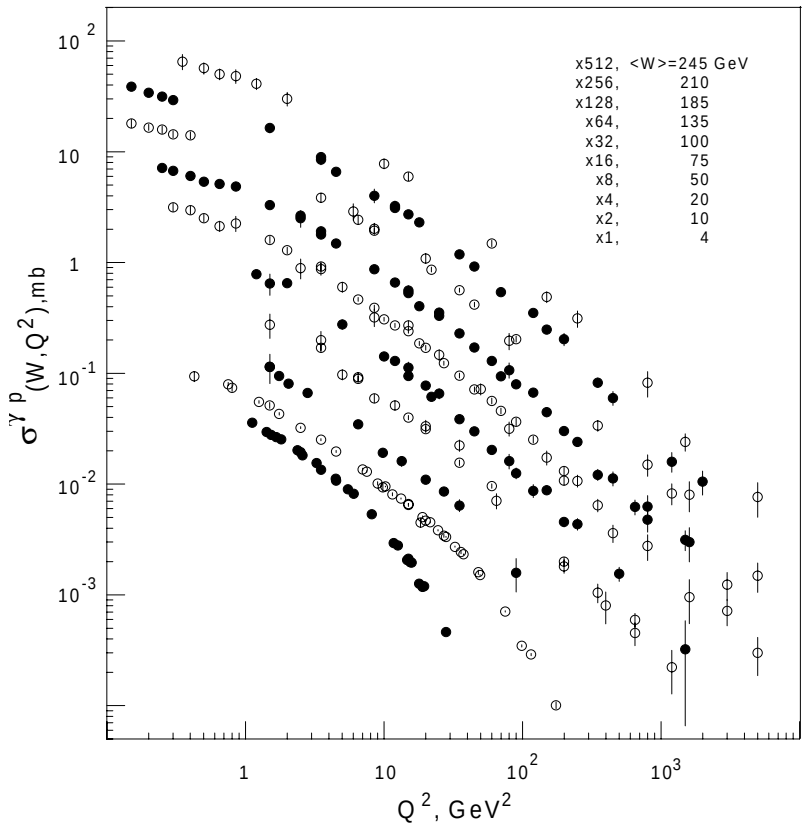

Fig. 1. Experimental data for $\sigma_T^{\gamma^* p}$ versus Q^2 at fixed W's showing a power decrease at high Q^2

we normalize elastic scattering amplitude $A(W^2, t, Q^2)$ with the external photons γ^* off mass shell. Thus

$$F_2^p(x,Q^2) = \frac{1}{4\pi^2\alpha} a(x,Q^2)\ \Im m A(W^2, t=0, Q^2). \quad (5)$$

The Regge model says nothing about the Q^2-dependence of the amplitude. The data (Fig. 1), however, suggest a power-like decrease of the cross-section at fixed W.

In the amplitude we take into account the contributions of a pomeron and of a secondary reggeon (f-reggeon).

$$A(W^2, t=0, Q^2) = P(W^2, Q^2) + F(W^2, Q^2). \quad (6)$$

Strictly speaking, an a_2-reggeon should also contribute to the $\gamma^* p$-amplitude (and is expected to be important at low energy). We do not include it in the fit to avoid extra free parameters and therefore we fit the model only in the region $W \geq 3$ GeV.

The f-reggeon contribution is written

$$F(W^2,Q^2) = iG_f(Q^2)\left(-i\frac{W^2}{m_p^2}\right)^{\alpha_f(0)-1}(1-x)^{B_f(Q^2)}, \quad (7)$$

where we take

$$G_f(Q^2) = \frac{g_f}{\left(1+Q^2/Q_f^2\right)^{D_f(Q^2)}},$$
$$D_f(Q^2) = d_{f\infty} + \frac{d_{f0}-d_{f\infty}}{1+Q^2/Q_{fd}^2}, \quad (8)$$

$$B_f(Q^2) = b_{f\infty} + \frac{b_{f0}-b_{f\infty}}{1+Q^2/Q_{fb}^2}. \quad (9)$$

As for the pomeron contribution, we take it in the form

$$P(W^2,Q^2) = P_1 + P_2, \quad (10)$$

with

$$P_1 = iG_1(Q^2)\mathcal{P}(W)(1-x)^{B_1(Q^2)},$$
$$P_2 = iG_2(Q^2)(1-x)^{B_2(Q^2)}, \quad (11)$$

$$G_i(Q^2) = \frac{g_i}{(1+Q^2/Q_i^2)^{D_i(Q^2)}},$$
$$D_i(Q^2) = d_{i\infty} + \frac{d_{i0}-d_{i\infty}}{1+Q^2/Q_{id}^2}, \qquad i=1,2, \quad (12)$$

$$B_i(Q^2) = b_{i\infty} + \frac{b_{i0}-b_{i\infty}}{1+Q^2/Q_{ib}^2}, \qquad i=1,2. \quad (13)$$

We would like to comment the above expressions. In spite of a seeming cumbersome form they are a direct generalization of the simplest parameterization of factors

$$G(Q^2) = \frac{g}{(1+Q^2/Q_0^2)^d} \qquad \text{and} \qquad (1-x)^b$$

with constant d and b in each term of the $\gamma^* p$-amplitude. A fit to experimental data shows that the parameters d and b should depend on Q^2.

Various models of the pomeron may be considered (via $\mathcal{P}(W)$), *e.g.*

Table 1. Experimental data used in the fit of DP and SCP models. Distribution of the partial χ^2's for each subset of data is illustrated for the DP model

Experiment, quantity	Number of points	Refs.	χ^2 in DP model
σ_T	99	[29]	122.79
($W \geq 3$ GeV)		[30]	
		[31]	
F_2^p			
($W \geq 3$ GeV)			
H1	93	[32]	67.42
H1	193	[33]	108.05
H1	44	[34]	39.18
ZEUS	188	[35]	233.70
ZEUS	34	[36]	22.20
BCDMS	175	[37]	285.40
NMC	156	[38]	175.40
E665	91	[39]	95.40
SLAC	136	[40]	167.50
Total	$N_p = 1209$		$\chi^2/d.o.f. = 1.11$

– **Dipole Pomeron (DP)**

$$\mathcal{P}(W) = \ln(-i\frac{W^2}{m_p^2}), \tag{14}$$

– **Supercritical Pomeron (SCP)**

$$\mathcal{P}(W) = \left(-i\frac{W^2}{m_p^2}\right)^{\alpha_P(0)-1}, \tag{15}$$

– **"Generalized" Pomeron**

$$\mathcal{P}(W) = \ln^{\mu}(-i\frac{W^2}{m_p^2}), \qquad 0 \leq \mu \leq 2. \tag{16}$$

We only investigate the first two models with a soft pomeron (here with an intercept close to one). In the DP model, the intercept of the pomeron is $\alpha_{\mathcal{P}}(0) = 1$, while in the SCP model, the pomeron intercept is fixed at its "world value" $\alpha_{\mathcal{P}}(0) = 1.0808$. Note that our SCP model is a generalization of the model by Donnachie and Landshoff [28] : we add in the amplitude a single term with a unit intercept.

The parameters must obey some restrictions to avoid unphysical situations (for example, the cross-section might become negative if we do not constrain $d_{2\infty} \geq d_{1\infty}$). These restrictions were taken into account when fitting (6-13) to the available experimental data.

In Table 1 we show details on the set of experimental data used for the determination of the parameters to analyze the properties of the model.

3 Results and discussion

3.1 Fit to the data

We performed a fit of the experimental data with the two models: the Dipole Pomeron and the Supercritical Pomeron. In the DP model, the Reggeon intercept was fixed at the value $\alpha_f(0) = 0.804$ obtained from hadronic reactions [26,27]. As regards to the SCP model only the intercept of Pomeron was fixed at the value $\alpha_{\mathcal{P}}(0) = 1.0808$ (we consider a "standard" soft Pomeron, though another value of $\alpha_{\mathcal{P}}(0)$ was obtained in [26,27]).

Table 2. Parameters obtained in the Dipole Pomeron model and in the Supercritical Pomeron model

	DP model	SCP model
Parameters	Value	Value
P_1-term		
μ	.10000E+01 (fixed)	
$\alpha_{\mathcal{P}}(0)$	.10000E+01 (fixed)	.10808E+01 (fixed)
$g_1(mb)$	.21898E-01	.10295E+00
$Q_1^2(GeV^2$	.15400E+02	.88709E+01
$Q_{1d}^2(GeV^2)$	.17852E+01	.15329E+01
$Q_{1b}^2(GeV^2)$	.33435E+01	.99243E+01
$d_{1\infty}$	.13301E+01	.13026E+01
d_{10}	.14370E+02	.89733E+01
$b_{1\infty}$	.21804E+01	.27830E+01
b_{10}	.42596E+01	.42832E+01
P_2-term		
$g_2(mb)$	-.99050E-01	-.78055E-01
$Q_2^2(GeV^2$	.34002E+02	.20269E+02
$Q_{2d}^2(GeV^2)$	.12327E+01	.22877E+01
$Q_{2b}^2(GeV^2)$	.20702E-01	.21626E-01
$d_{2\infty} - d_{1\infty}$	.00000E+00 (fixed)	.00000E+00 (fixed)
d_{20}	.22607E+02	.72161E+01
$b_{2\infty}$	.24686E+01	.30767E+01
b_{20}	.17023E+03	.25000E+03
F-term		
$\alpha_f(0)$	.80400E+00 (fixed)	.71369E+00
$g_f(mb)$	.29065E+00	.18189E+00
$Q_f^2(GeV^2$	.29044E+02	.22469E+02
$Q_{fd}^2(GeV^2)$	.54462E+00	.13003E+00
$Q_{fb}^2(GeV^2)$	.20656E+01	.49263E+01
$d_{f\infty}$	.13554E+01	.12940E+01
d_{f0}	.75127E+02	.22533E+03
$b_{f\infty}$	.27239E+01	.32140E+01
b_{f0}	.64713E+00	.00000E+00(fixed)
$\chi^2/d.o.f.$	1.11	1.15

The corresponding χ^2 and the fitted parameters are given in Tables 1, 2. Both models describe well the data. In practice, they give plots which coincide in the region of the fitted experimental data; they become different only in the very far asymptotics or, as anticipated, at low W-values. We plot $\sigma_T^{\gamma^* p}(W, Q^2)$ in Figs. 2, 3 and $F_2^p(x, Q^2)$ in Figs. 4 – 7; our DP results are compared to ALLM ones [17], recalculated after corrections of a few misprints [41]. In what follows we concentrate mainly on a discussion of the DP model.

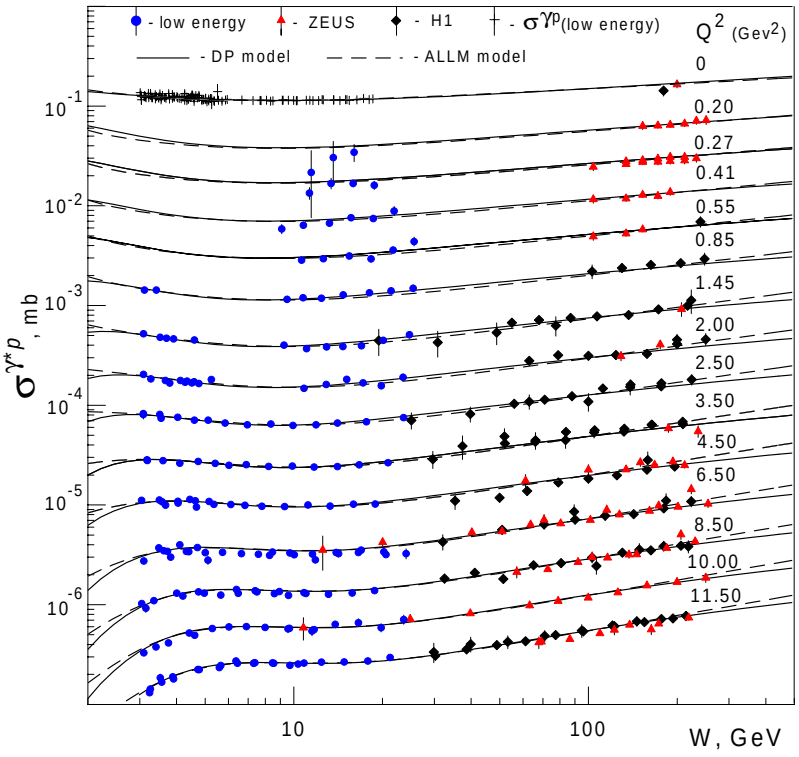

Fig. 2. Experimental data for $\sigma^{\gamma^* p}(W, Q^2)$ at low Q^2 and description in our model and ALLM model [17]. A factor of 2^{k-1} for each curve is omitted (k is the number of the curve starting from the top). Other notations are given in the figure

3.2 (γ, p) cross-section (at $Q^2 = 0$)

In the DP model, from (5)-(14) we obtain

$$\sigma_T^{\gamma p}(W) = g_1 \ln\left(\frac{W^2}{m_p^2}\right) + g_2 + g_f \cos\left(\frac{\pi}{2}(\alpha_f(0) - 1)\right)\left(\frac{W^2}{m_p^2}\right)^{(\alpha_f(0)-1)}. \quad (17)$$

The existing data on the cross section for a real photon-proton interaction are not precise enough to determine unambiguously the coupling constants g_1, g_2, g_f and the intercept $\alpha_f(0)$ (this is why we fixed the f-reggeon intercept). The behaviour (mild rise) of $\sigma_T^{\gamma p}(W)$ is shown in Fig. 2.

We would like to comment on the properties of the models we investigated at $Q^2 = 0$. As usual in a multiparametric problem there are several minima of χ^2. We found one of them with $\chi^2/d.o.f. = 1.07$ which is significantly better than in the one given here. In this solution, which we did not retain, the values of $\sigma_T^{\gamma^* p} \sim 0.19$ mb at the HERA energies are slightly higher than the experimental points. At the same time as noted in [43] an extrapolation of the ZEUS BPC data to $Q^2 = 0$ gives exactly this value of $\sigma_T^{\gamma^* p}$.

3.3 Partial contributions to the (γ^*, p) cross section

Let us remark about the negative sign found for the parameter g_2 (see Table 2). The same situation takes place for pp and $\bar{p}p$ cross-sections [26,27], where a negative contribution plays an important role for a good description of the subasymptotic elastic scattering data. At low energy it is compensated by the f-reggeon contribution and at high energy by the rising term P_1 of the pomeron contribution.

Possibly this negative term can take into account the multipomeron exchanges contribution. An argument in favor of this point of view (rather than a proof) holds when we consider the following simple model used in crude discussions .Let

$$A^{(1)}(s,t) = i(a\xi + b)e^{(R^2 + \alpha'\xi)t}, \quad \xi = \ln(-is/s_0)$$

be the contribution of a double $j-$pole (the first term) and of a simple pole (the second term) in the elastic scattering amplitude. The amplitude of the two-pomerons exchange in the eikonal approximation at $t = 0$ is

$$A^{(2)}(s,0) = -i\frac{(a\xi + b)^2}{32\pi(R^2 + \alpha'\xi)} \approx -\frac{i}{8\pi}[\xi\alpha'(a/2\alpha')^2 + (a/2\alpha')(b - R^2 a/2\alpha')],$$

in the high energy approximation. Thus for $A(s,0) = A^{(1)}(s,0) + A^{(2)}(s,0)$ we find an energy dependence of the form

$$A(s,0) \approx i(\tilde{a}\xi + \tilde{b}).$$

One can see that the new terms $(\tilde{a}, \tilde{b})$ in $A(s,0)$ can be respectively positive and negative by a natural choice of the positive constants a, b.

In the SP model an interpretation of the constant term is less clear, however its sign follows from the fit to data. In

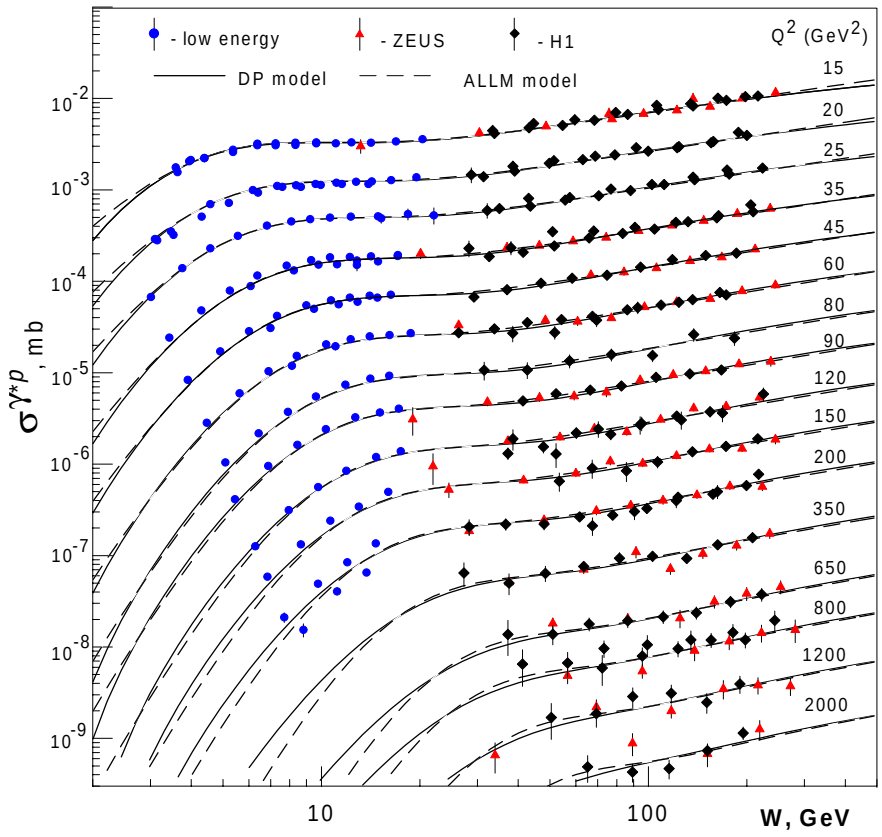

Fig. 3. Same as in Fig. 2 for intermediate and high Q^2

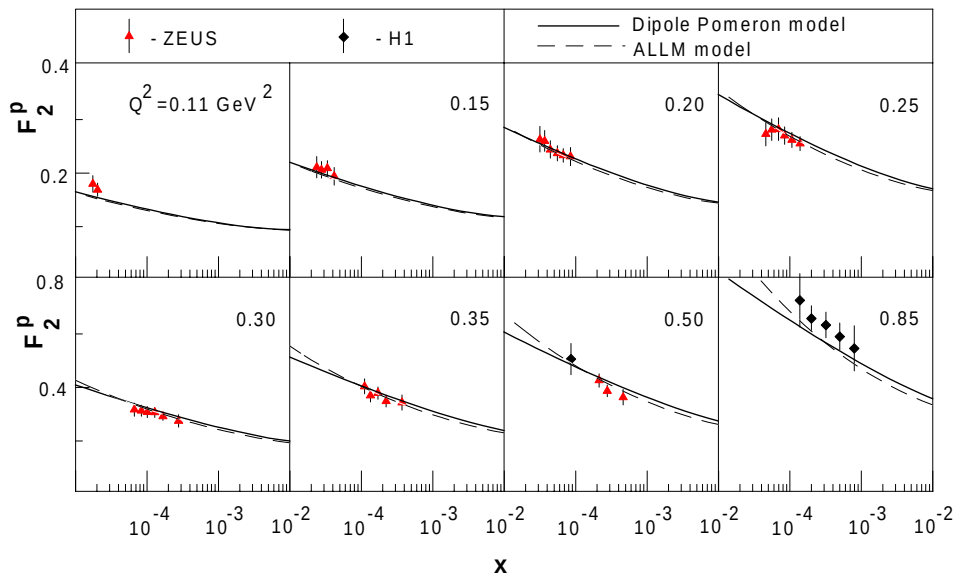

Fig. 4. Experimental data for the proton structure function $F_2^p(x, Q^2)$ at low Q^2 and predictions in the Dipole Pomeron model and in ALLM model. All notations are given in the figure

any case we think that due to complicated interference of the positive terms (from $F(x, Q^2)$ and $P_1(x, Q^2)$) with the negative term (from $P_2(x, Q^2)$), it is possible to describe $\sigma_T^{\gamma^* p}(W, Q^2)$ and $F_2^p(x, Q^2)$ without a Q^2-dependent pomeron intercept.

In order to see how quickly the asymptotic regime is reached in the DP model, we plot versus W in Fig. 8 the ratios of contributions in the cross-section $\sigma_T^{\gamma^* p}(W, Q^2)$ due to the subasymptotic terms $F(W, Q^2)$ and $P_2(W, Q^2)$ to the asymptotic one $P_1(W, Q^2)$ at some fixed values of Q^2. One can see that the asymptotic domain (where P_1 dominates) occurs for high W and moreover, is shifted to even higher W's while Q^2 rises. This proves that it may be incorrect to draw conclusions on F_2^p in term of its asymptotic contribution.

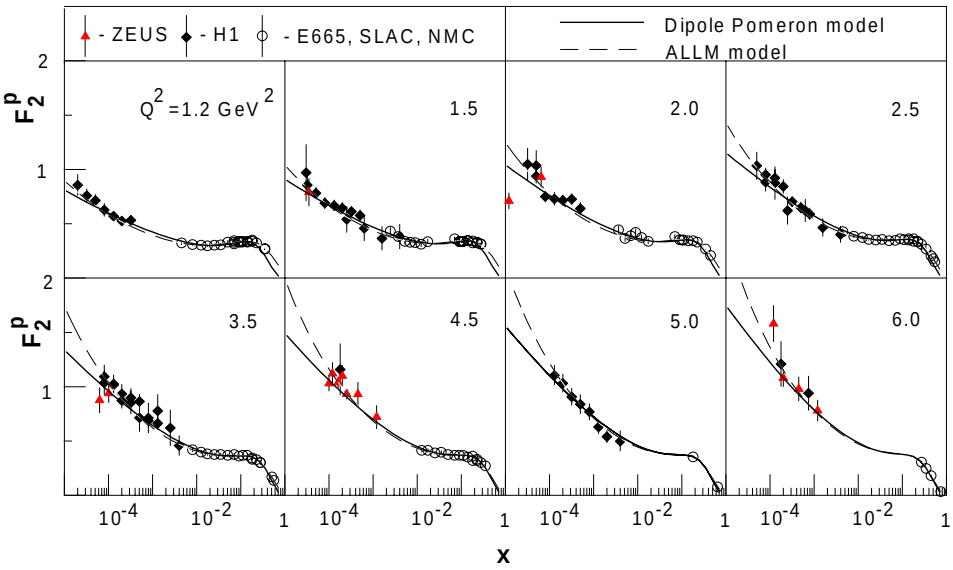

Fig. 5. Same as in Fig. 4

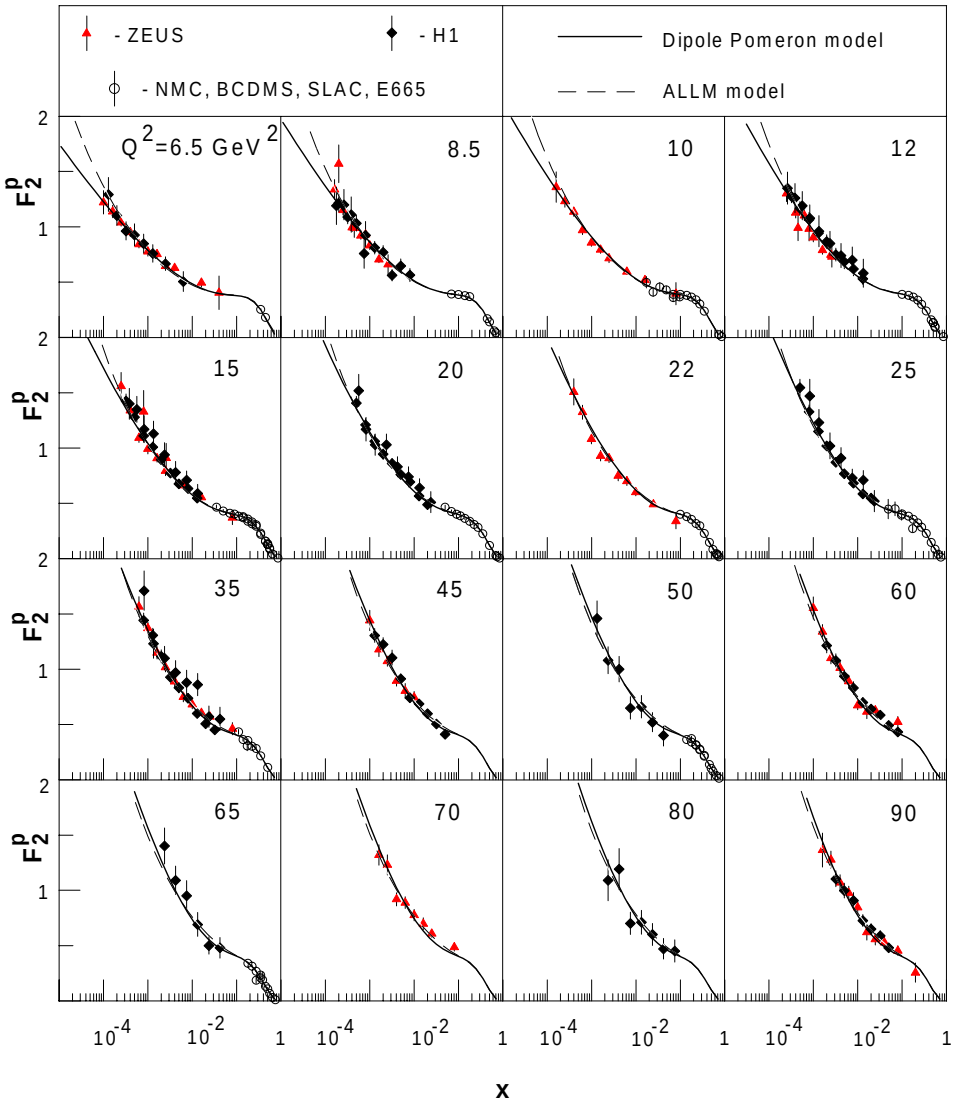

Fig. 6. Same as in Fig. 4 for intermediate and high Q^2

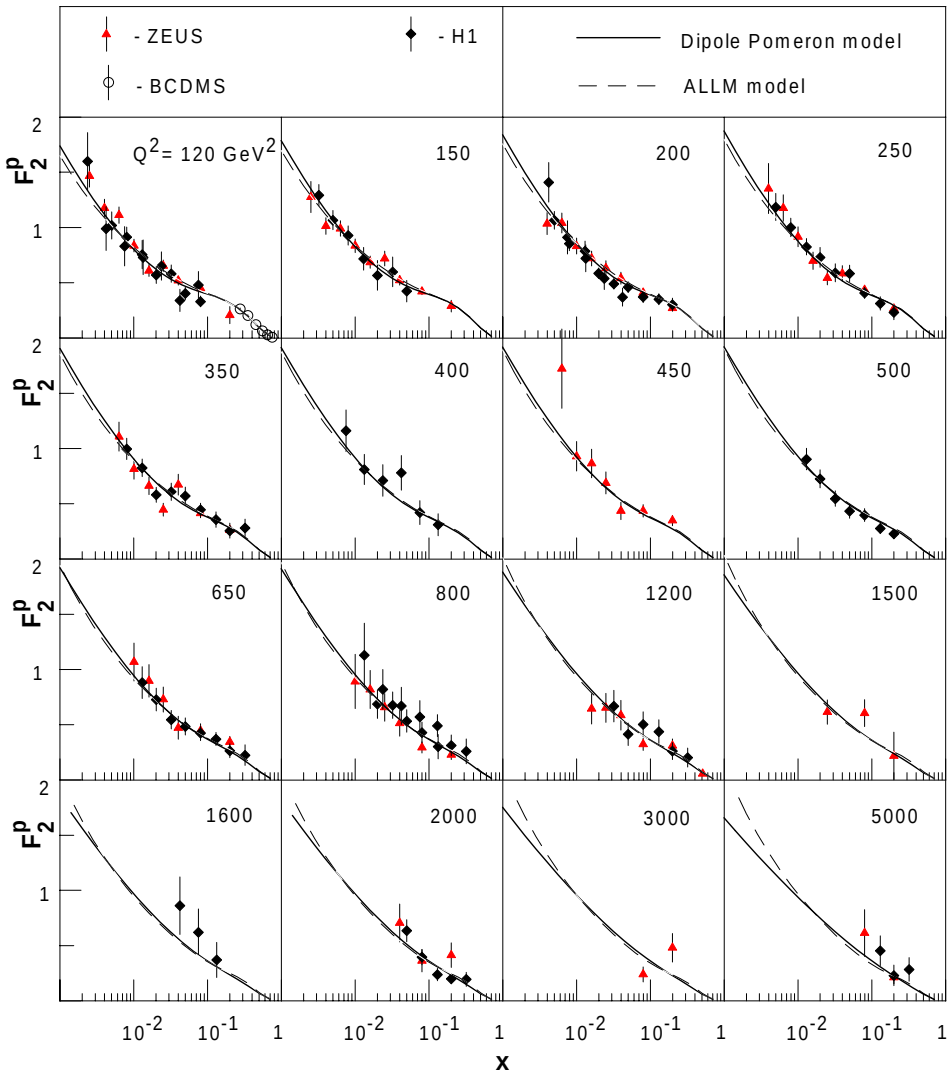

Fig. 7. Same as in Fig. 4 at high Q^2

3.4 Comparison with other models

As noted above, models with $F_2^p \propto \ln(1/x)$ at $x \ll 1$, can be interpreted as taking into account a Dipole Pomeron (with a unit intercept) contribution to the SF. In Table 3 for two of them, namely BH [23] and ScSp [24], we compare the quality of their description of the data (measured here with χ^2/(number of points)) with those obtained in the DP (present work) and ALLM [17] models. The free parameters in all models were (re)determined by fitting our set of data (for each model we selected the kinematical region of W, Q^2, x as indicated by the authors). For ALLM and for our model we give the partial χ^2-s.

Because we describe $\sigma_T^{\gamma^* p}$ (orF_2^p) in the whole kinematical region (the only restriction $W > 3$ GeV is imposed), we can compare our model with the ALLM model [17] (where the only restriction is $W > 2$ GeV). We obtain a very small difference in the whole region where data exist, though there is a quite different trend outside the experimental range (see Figs. 2 – 7). Thus, future experiments at lower x should be crucial to test the existing models and as a guide for constructing more sophisticated models.

Table 3. Comparison of the quality of data description by various models (measured here with χ^2/(number of points))

Kinematical region	N of points	ALLM [17]	ScSp [24]	BH [23]	DP model
$W > 3$ GeV	1209	1.061	-	-	1.089
$Q^2 \leq 350$ GeV^2 $W \geq 60$ GeV	329	0.81	1.098	-	0.77
$Q^2 \geq 5$ GeV^2 $x \leq 0.05$	227	0.89	-	1.04	0.79

3.5 $x-$slope or $\partial ln F_2^p(x,Q^2)/\partial ln(1/x)$

The data suggest an interesting tendency in the behaviour of $F_2^p(x,Q^2)$ at small x and rising Q^2. It concerns the sharp increase of F_2 as x decreases for a large span of Q^2 values (sometimes called the HERA effect). When Q^2 rises around $Q^2 \sim 200 - 500$ GeV^2, the fast growth of F_2^p with decreasing x slows down and as Q^2 increases further is reversed. This effect (let us call it damping of the HERA effect) is very weak from the experimental point

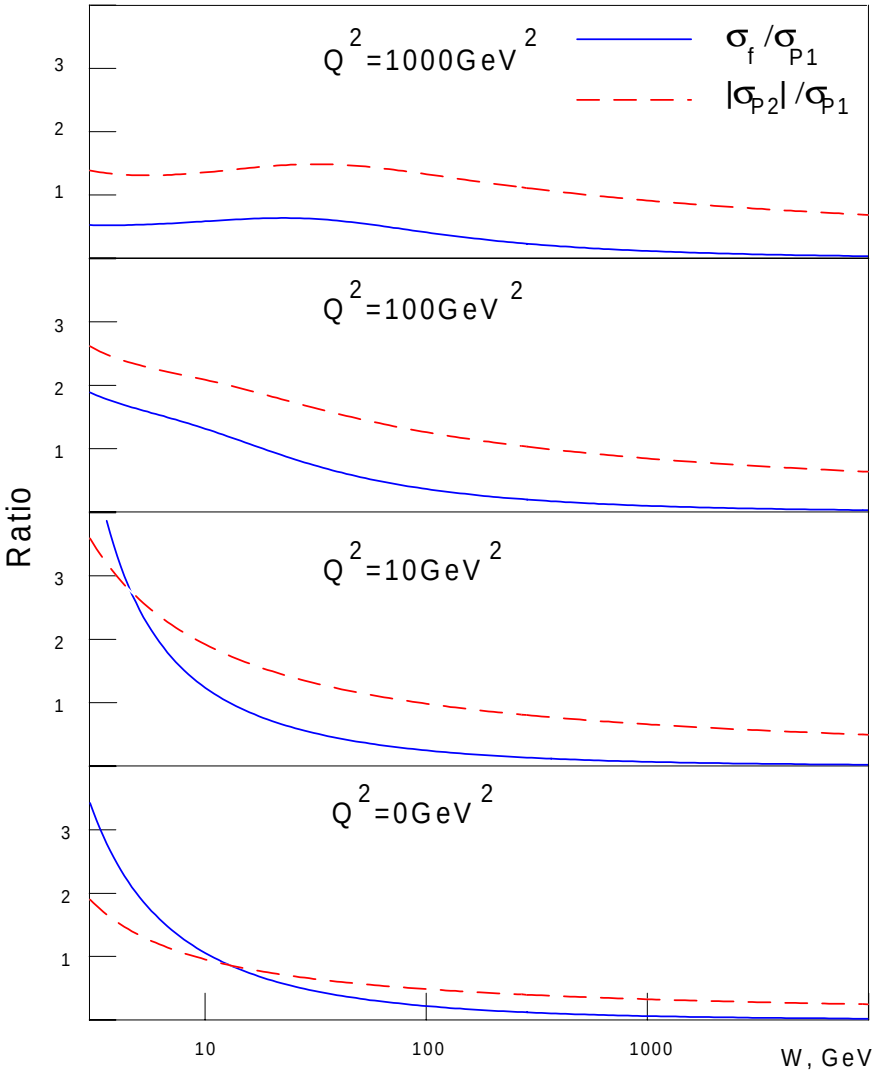

Fig. 8. Ratios of P_2- and F- terms to P_1-term in cross-section $\sigma_T^{\gamma^* p}(W, Q^2)$ versus W at various fixed Q^2 as indicated

of view because lacking of a sufficient number of data at high Q^2. Nevertheless, one can see it (or simply constant that it does not contradict the available experiments) *e.g.* in the Fig. 7. In spite of the very qualitative character of the experimental observation, the following quantitative confirmation holds. The x-slope of the proton SF

$$B_x(x, Q^2) = \partial \ln \left(F_2^p(x, Q^2)\right) / \partial \ln(1/x), \qquad (18)$$

is strongly model dependent. As an example, we examine B_x in three models for which the behaviour of the rise of F_2 with decreasing x can accommodate all existing data : the Dipole Pomeron model (see above), the ALLM model [17] and the recent model [44] (hereafter labeled LKP). The asymptotic behaviour (when $Q^2 \to \infty$ and $x \ll 1$) of this slope is successively

$$B_x^{(DP)}(x \ll 1, Q^2 \to \infty) \approx \frac{1}{\ln(Q^2/x)},$$

$$B_x^{(ALLM)}(x \ll 1, Q^2 \to \infty) \approx \Delta(Q^2) = a\left(1 - 1/\ln\ln(\frac{Q^2}{\Lambda^2})\right),$$

$$B_x^{(LKP)}(x \ll 1, Q^2 \to \infty) \approx \frac{1}{2}\sqrt{\gamma_1 \ln\ln\frac{Q^2}{Q_0^2} \;/\; \ln\frac{x_0}{x}}\ ,$$

where $a, \Lambda, Q_0, \gamma_1, x_0$ are parameters of the models. The slope $B_x(x, Q^2)$ is plotted versus Q^2 for the DP model in Fig. 9(a) for several x's as indicated. In Figs. 9(b,c) the $x-$slope for the ALLM and LKP models is plotted for comparison.

It should be noted that the $x-$slope, at the largest experimental Q^2, is far from asymptotics in all models. Our DP model predictions differ strongly from those obtained in the ALLM model, where the intercept $\Delta(Q^2)$ goes to a constant independent on x at $Q^2 \to \infty$, and from those in the LKP model, where B_x rises infinitely when $Q^2 \to \infty$. However in the domain of Q^2 slightly above the existing data, the DP and LKP models are in qualitative agreement, together predicting a decreasing B_x. They both predict the damping of the HERA effect, illustrated by the presence of a maximum when plotting B_x versus Q^2 for a given low x (Fig. 9). New experimental data in this kinematical region would certainly help to verify if this phenomenon does exist at $100 \lesssim Q^2 \lesssim 1000 GeV^2$.

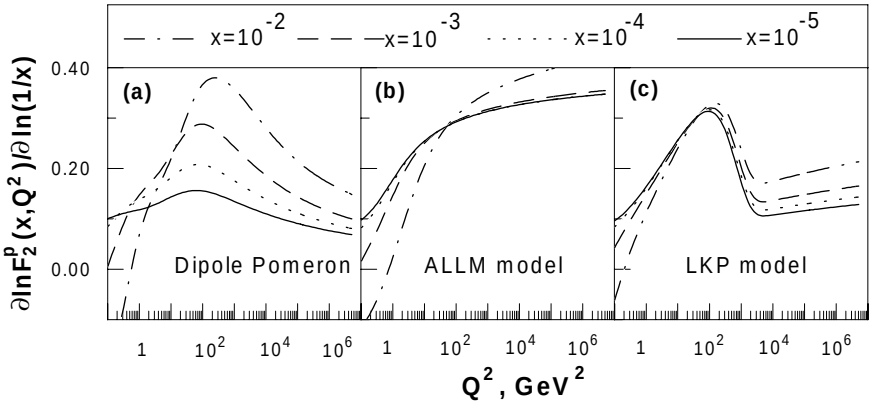

Fig. 9. The x-slope of F_2^p as function of Q^2 at the four fixed x in the DP, ALLM [17] and LKP [44] models

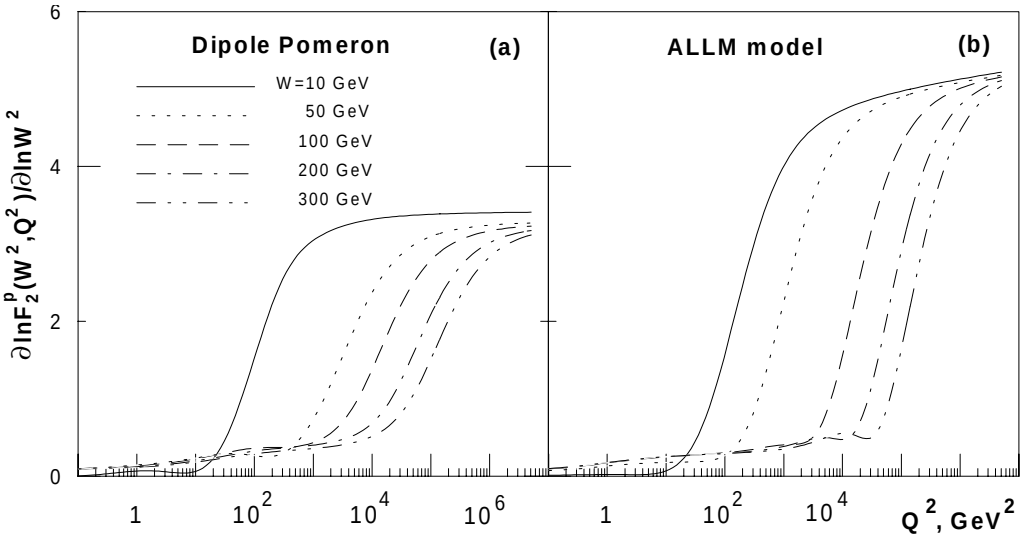

Fig. 10. The W-slope of F_2^p as function of Q^2 at the various fixed W in the DP (a) and ALLM [17] (b) models

3.6 $x-$ and $W-$ slopes and "effective intercept"

We would like to emphasize that an apparent contradiction of the constant and "small" pomeron intercept (=1) in the DP model with the "experimentally" established conclusion about the "high" (and rising with Q^2) value of $\delta(Q^2)$, where δ is the power in a small-x behaviour of the SF, $F_2^p(x,Q^2) \propto x^{-\delta(Q^2)}$, is not a real contradiction. On the one hand, the conclusion is based on a simplified fit that takes into account only the asymptotic contribution to the SF. On the second hand, the $x-$slope (18), i.e. $\partial \ln F_2^p(x,Q^2)/\partial \ln(1/x)$, rather than an "effective intercept" was determined. To show the difference we define the effective intercept $\Delta^{(eff)}$ by rewriting F_2^p in the general form

$$F_2^p(x,Q^2) = G(Q^2)\left(\frac{1}{x}\right)^{\Delta^{(eff)}(x,Q^2)}, \qquad (19)$$

with

$$\Delta^{(eff)}(x,Q^2) = \alpha_{\mathcal{P}}^{(eff)}(x,Q^2) - 1\ . \qquad (20)$$

Note that $\Delta^{(eff)}(x,Q^2) = B_x(x,Q^2)$ only if $\Delta^{(eff)}(x,Q^2)$ in (19) does not depend on x, however in general an effective intercept does not coincide with x-slope.

Because there are three variables Q^2, x, W^2 with only two of them being independent, the SF can be considered as a function of Q^2 and W^2. Consequently a $W-$slope of the proton SF

$$B_W = \partial \ln F_2^p(W^2,Q^2)/\partial \ln W^2 \qquad (21)$$

as well as an effective intercept $\Delta^{(eff)}(W^2,Q^2)$ should be defined. Again the difference between B_W and $\Delta^{(eff)}$ is important if $\Delta^{(eff)}$ depends on W^2.

One can see from Fig. 9 that $x-$slopes increase with Q^2 up to a few hundreds of GeV^2. A similar growth of B_W is demonstrated in the Fig. 10a (the behaviour of B_W in the ALLM model is shown in the Fig. 10b for comparison). A sharp growth of B_W at large Q^2 is due to the influence of the factors $(1-x)^{B_i(Q^2)}$ in (7) and (11) which become very important at $Q^2 \gtrsim W^2$ (or $x \approx 1$)). In both cases (B_x and B_W) the subasymptotic terms P_2 and F contribute mainly in a wide region of Q^2.

So we would like to stress once more that as follows from the above arguments the preasymptotic contributions to the SF are important (at least for Dipole Pomeron and Supercritical Pomeron models) even in the HERA kinematical region.

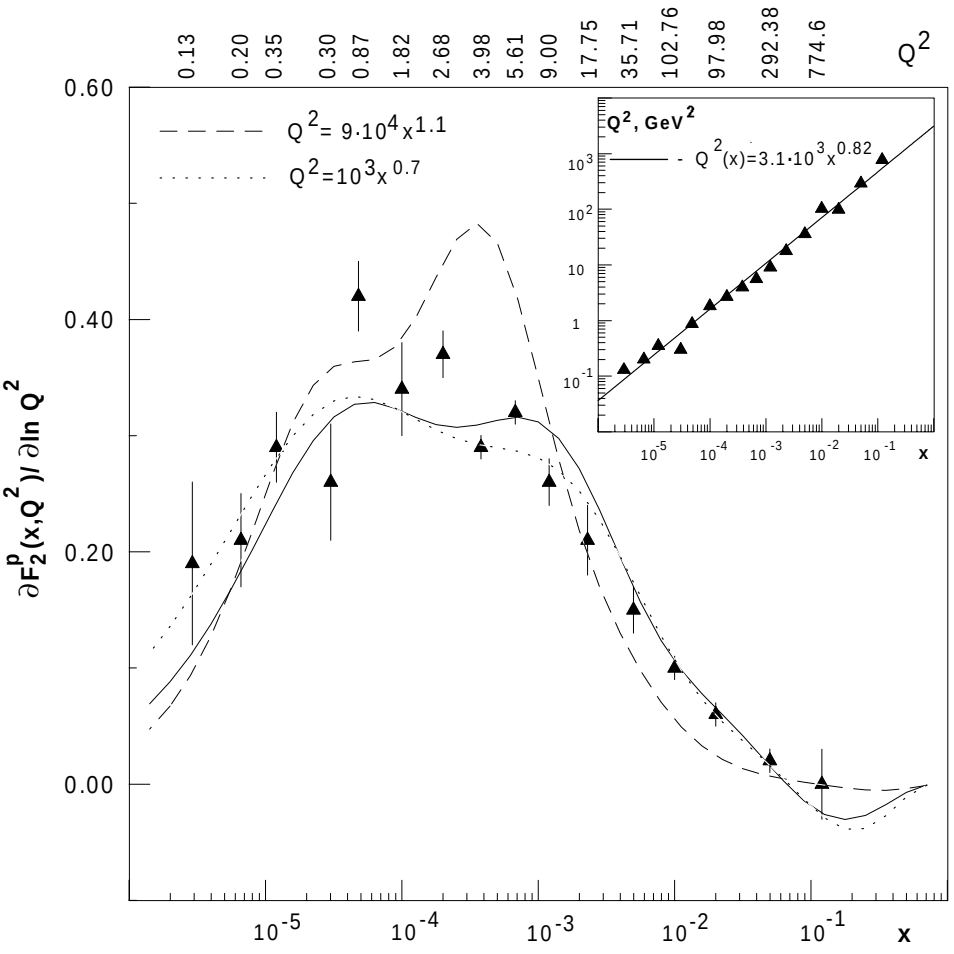

Fig. 11. Slope $B_Q(x,Q^2)$. Experimental data from HERA and results of calculation in the Dipole Pomeron model. Curves correspond to the different choice of line $Q^2(x)$ (see the text)

As concerned the effective intercepts, it follows from (5)-(14) that in DP model at $Q^2 \to \infty$ and small fixed x

$$F_2^p(x,Q^2) \approx \frac{1}{4\pi^2\alpha} Q^2 G_1(Q^2) \ln W^2$$
$$\approx \frac{1}{4\pi^2\alpha} Q^2 G_1(Q^2) \ln(\frac{Q^2}{x}).$$

Identifying with (19), one gets $G(Q^2) = \frac{1}{4\pi^2\alpha} Q^2 G_1(Q^2)$ and

$$\Delta^{(eff)}(x,Q^2) \approx \frac{\ln\ln(Q^2/x)}{\ln(1/x)}.$$

Thus in the Dipole Pomeron model the effective intercept $\Delta^{(eff)}(x,Q^2)$ is rising with rising Q^2 and is decreasing with decreasing x, at least for large Q^2 and small x. Similarly one can find that in the kinematical region $W^2 \gg Q^2$ ($x \ll 1$) where P_1-term dominates

$$\Delta^{(eff)}(W^2,Q^2) \approx \frac{\ln\ln W^2}{\ln W^2}.$$

However we note that the effective intercept is not a very convenient parameter for analysing the experimental data because its definition is model dependent (see the factor $G(Q^2)$ in (19)).

3.7 $Q-$slope or $\partial F_2^p(x,Q^2)/\partial ln Q^2$

Recently, new low x data from HERA have been reported [42,43] and discussed [17,44,45], concerning the logarithmic Q^2 derivative of F_2^p (for brevity called $Q-$slope)

$$B_Q(x,Q^2) = \frac{\partial F_2^p(x,Q^2)}{\partial \ln Q^2}. \qquad (22)$$

A "$Q-$slope effect" presented as a new phenomenon has been attributed to these data, it is illustrated in Fig. 11: the data exhibit a peak at $Q_0^2 \sim 1-5$ GeV^2. Also shown in the figure, are the results of a calculation within our DP model, which is a pure Regge one; quite a good agreement with the data for both sides of the peak is obtained.

The peak is currently interpreted as a transition region from a Regge behaviour (at $Q^2 \lesssim Q_0^2$) to a perturbative QCD regime (at $Q^2 \gtrsim Q_0^2$). However we emphasize that such a value of Q_0^2 is imposed by the specified selection of experimental points, or in other words with [44] by the particular (experimentally constrained) path ($Q^2(x)$) chosen on the surface representing B_Q in the 3 dimensions space. Consequently, an unbiased determination of the transition region requires a study of the submits of this surface and may yield Q_0^2, depending on x, and very different from $1-5$ GeV^2 (it has been found $Q_0^2(x \ll 1) \sim 40$ GeV^2 in [44]).

In the mini-plot at the upper right corner of the Fig. 10 we show the data positions in a (x, Q^2)-plane together with a line $Q^2 = 3.1 \cdot 10^3\ x^{0.82}$ which is fitted to the data. Solid line in the Fig. 10 corresponds to B_Q calculated in the DP model along this path.

Let us connect x and Q^2 by some analytical dependence $Q^2 = Q^2(x)$ that lies within a physical region on (x, Q^2)-plane. This region is bounded by the condition

$$y = \frac{Q^2}{x(s - m_p^2)} \leq 1.$$

For HERA experiments, the c.m.s. energy is $\sqrt{s} \approx 300$ GeV and this condition writes Q^2 (in GeV^2) $< 9 \cdot 10^4\ x$. As examples, we have calculated also $B_Q(x, Q^2)$ for two arbitrary dependencies satisfying the above condition : $Q^2 = 9 \cdot 10^4\ x^{1.1}$ and $Q^2 = 10^3 x^{\ 0.7}$. The results are given in Fig. 10 and show that the positions of the peaks in x differ at least by an order of magnitude. By an appropriate choice of the curve $Q^2(x)$ the difference can be enforced. Thus, a peak indeed exists but its position is strongly dependent on the choice of experimental data. Undoubtedly, the $Q-$slope effect has to be investigated in more details from the experimental and theoretical points of view.

4 Conclusion

In our opinion the most interesting and important message of that paper is the following. All available data on the proton structure function at $W > 3$ GeV can be described in the framework of the traditional Regge approach with a soft pomeron and an appropriate Q^2-dependence of the residue function. It is not necessary for this aim to use an high intercept similar to the "Born" hard BFKL Pomeron intercept or a Q^2-dependent intercept. We find that the main difficulty is the extension of the kinematical domain, where the pomeron is successfully applied, from the small $x \ll 1$ to the large $x \sim 1$ rather than the choice of the specified pomeron singularity (in the j-plane) and its intercept. It means that the subasymptotic contributions are extremely important not only at low W but also at HERA energy and even at more high energies (for the DP model it is illustrated in the Figs. 4,5).

We note that in the DP model the "effective intercept" rises infinitely when Q^2 rises and goes to zero when x decreases.

At the same time, the model predicts a new phenomenon in the behaviour of the slope $B_x(x, Q^2)$. Namely the observed rising growth of the $x-$slope of F_2^p, at small x and high Q^2, will come to stop and then will begin to decrease at highest Q^2. This phenomenon corresponding to a damping of the HERA effect requires a further investigation.

Acknowledgements. We are grateful to E. Predazzi for reading the manuscript. We thank M. Giffon and M. Bertini for valuable discussions.

References

1. M. Bertini et al., Rivista Nuovo Cimento **19**, 1 (1996)
2. A. Levy, DESY 97-013, 1997 (unpublished)
3. Yu.L. Dokshitzer, Sov. Phys. JETP **46**, 641 (1977); L.V. Gribov, E.M. Levin, M.G. Ryskin, Phys. Rep. **100**, 1 (1983); L.N. Lipatov in *Perturbative Quantum Chromodynamics*, ed. by A.H. Mueller (World Scientific, Singapore 1989); G. Altarelli, G. Parisi, Nucl. Phys. B **126**, 298 (1977)
4. E. Levin, TAUP 2435-97; hep-ph/9706448, 1997 (unpublished)
5. E. Levin, DESY 97-171; hep-ph/9709226, 1997 (unpublished)
6. Y.Y. Balitskii, L.N. Lipatov, Sov. Phys. JETP **28**, 822 (1978); E.A. Kuraev, L.N. Lipatov, V.S. Fadin, ibid **45**, 199 (1977); L.N. Lipatov, ibid **63**, 904 (1986)
7. V.S. Fadin, L.N. Lipatov, DESY 98-033; hep-ph/9802290, 1998 (unpublished)
8. A.L. Ayala Filho, M.B. Gay Ducati, E.M. Levin, DESY 97-212; hep-ph/9710539, 1997 (unpublished)
9. E. Gotsman, E.M. Levin, U. Maor, DESY 97-154; hep-ph/9708275, 1997 (unpublished)
10. M. Glük, E. Reya, A. Vogt, Zeit. Phys. C **67**, 433 (1995); V. Barone, M. Genovese, N.N. Nicolaev, E. Predazzi, B.G. Zakharov, Zeit. Phys. C **70**, 83 (1996)
11. A.D. Martin, R.G. Roberts, W.J. Stirling, Phys. Lett. B **387**, 419 (1996)
12. H.L. Lai et al. (CTEQ Collaboration), Phys. Rev. D **51**, 4763 (1996)
13. Z. Huang, H. Jung Lu, I. Sarcevic, AZPH-TH/97-07; hep-ph/9705250, 1997 (unpublished)
14. V.A. Petrov, Nucl. Phys. (Proceedings Suppl.) A **54**, 160 (1997)
15. A. Capella et al., Phys. Lett. B **349**, 561 (1995)
16. H. Abramovicz et al., Phys. Lett. B **269**, 465 (1991)
17. H. Abramovicz, A. Levy, DESY 97-251; hep-ph/9712415, 1997 (unpublished)
18. P. V. Landshoff, in *Proceedings of the summer school on hadronic aspects of collider physics, uoz, 1994*, ed. by E.P. Locher (Villigen, PSI-Proceedings 94-01, 1994), p. 135
19. M. Bertini, M. Giffon, E. Predazzi, Phys. Lett. B **349**, 561 (1995)
20. K. Adel, F. Barreiro, F.J. Ynduráin, Nucl. Phys. B **495**, 221 (1997)
21. E. Martynov, in *Proceedings of the workshop on soft physics "Hadrons-94", Uzhgorod, Ukraine, September 1994*, ed. by G. Bugrij, L. Jenkovszky, E. Martynov (Kiev, 1994), p. 311; in *Proceedings of the VI Blois Conference on Elastic and Diffractive Scattering, Blois, France, June 1995*, ed. by P. Chiapetta, M. Haguenauer, J.Trân Thanh Vân (Editions Frontières 1996), p. 203
22. L. Jenkovszky, E. Martynov, F. Paccanoni, PFPD 95/TH/21, Padova University, 1995 (unpublished)
23. W. Buchmüller, D. Haidt, DESY 96-061; hep-ph/9605428, 1996 (unpublished)
24. D. Schildknecht, H. Spiesberger, BI-TP97/25; hep-ph/9707447, 1997 (unpublished)
25. P. Desgrolard et al., Phys. Lett. B **309**, 191 (1993)
26. P. Desgrolard et al., Nuovo Cimento A **107**, 637 (1994)
27. P. Desgrolard, M. Giffon, E. Martynov, Nuovo Cimento A **110**, 537 (1997)

28. A. Donnachie, P.V. Landshoff, Zeit. Phys. C **61**, 139 (1994)
29. S.I Alekhin et al., CERN-HERA 87-01, 1987
30. ZEUS Collaboration, M. Derrick et al., Zeit. Phys. C **63**, 391 (1994)
31. H1 Collaboration, S. Aid et al., Zeit. Phys. C **69**, 27 (1995)
32. H1 Collaboration, T. Ahmed et al., Nucl. Phys. B **439**, 471 (1995)
33. H1 Collaboration, S. Aid et al., Nucl. Phys. B **470**, 3 (1996)
34. H1 Collaboration, C. Adolf et al., Nucl. Phys. B **497**, 3 (1997)
35. ZEUS Collaboration, M. Derrick et al., Zeit. Phys. C **72**, 399 (1996)
36. ZEUS Collaboration, J. Breitweg et al., Phys. Lett. B **407**, 432 (1997)
37. BCDMS Collaboration, A.C. Benvenuti et al., Phys. Lett. B **223**, 485 (1989)
38. NMC Collaboration, M. Arneodo et al., Nucl. Phys. B **483**, 3 (1997)
39. E665 Collaboration, M.R. Adams et al., Phys. Rev. D **54**, 3006 (1996)
40. L.W. Whitlow et al., Phys. Lett. B **282**, 475 (1992); L.W. Whitlow, SLAC-357, 1990 (unpublished)
41. we thank H. Abramovicz for explaining comments relative to [17]
42. A. Caldwell, Invited talk in the DESY Theory Workshop (October 1997)
43. L. Bauerdick, Talk at the Max Planck workshop, Heidelberg (1997)
44. P. Desgrolard, L. Jenkovszky, F. Paccanoni, LYCEN 9808; hep-ph/9803286, 1988 (unpublished); P. Desgrolard, L. Jenkovszky, F. Paccanoni, in *Proceedings of the 6^{th} workshop on Deep Inelastic Scattering and QCD*, Brussels 1998 (in press)
45. E. Gotsman, E. Levin, U. Maor, TAUP 2471/97; hep-ph/9712517, 1997 (unpublished)